Ultrasound Backscatter Microscopy/Spectroscopy and Optical Coherence (Doppler) Tomography for Mechanism-Specific Monitoring of Photodynamic Therapy *in vivo* and *in vitro*

Victor X.D. Yang[1,3,4], Greg J. Gzarnota[3,4], I. Alex Vitkin[1,2,4], Mike Kolios[1,4], Michael Sherar[1,2,4], Johanes de Boer[5], Bruce Tromberg[5], Brian C. Wilson[1,2,4]

Departments of [1]Medical Biophysics, [2]Radiation Oncology, [3]Faculty of Medicine, University of Toronto, and [4]Ontario Cancer Institute/Princess Margaret Hospital, University Health Network, Toronto, ON, M5G2M9, Canada
[5]Beckman Laser Institute and Medical Clinic,
University of California Irvine, Irvine, CA, 92612 USA

Abstract

Photodynamic therapy (PDT) can induce a variety of tissue changes, including apoptosis, oncosis, and vascular responses. A preliminary study using two non-invasive imaging techniques, ultrasound backscatter microscopy/spectroscopy (UBM/UBS) and optical coherence/Doppler tomography (OCT/ODT), is presented. Photofrin PDT of melanoma was studied using a mouse model and imaged by both modalities *in vivo*. Post PDT, increase in the signal intensity and change in the backscatter spectrum were observed in UBM/UBS. A transient increase in the signal attenuation was observed by OCT and changes in the neovasculular blood flow were detected using ODT. Additional *in vitro* experiments were performed to examine the possible causes of the observed signal changes.

Keywords: photodynamic therapy; imaging; monitoring; apoptosis; oncosis; necrosis; blood flow

*Correspondence: wilson@uhnres.utoronto.ca Tel: 416-946-2952

Introduction

Photodynamic therapy (PDT) is rapidly coming into clinical use for both oncological [1] and other conditions [2,3]. PDT uses light-activated drugs to destroy or modify diseased tissues, mediated by photochemical generation of cytotoxic singlet oxygen [4]. The dosimetry of PDT is complex, involving a combination of light 'dose', photosensitizer concentration, and local tissue pO_2 that vary dynamically and interdependently during irradiation [5,6]. There are also multiple mechanisms of tissue damage: cell deaths due to necrosis (oncosis) or apoptosis; a (micro) vascular response and immunological factors. Hence, there is considerable need to develop methods to enable the monitoring of the various tissue responses after (and, ideally, also during) treatment. It would be of potential advantage if the monitoring methods could discriminate between the different mechanisms of tissue and cellular damage.

Optical Methods for Tumor Treatment and Detection: Mechanisms and Techniques in Photodynamic Therapy XI, Thomas J. Dougherty, Editor, Proceedings of SPIE Vol. 4612 (2002) © 2002 SPIE · 1605-7422/02/$15.00

Previously, we have reported initial studies of minimally-invasive PDT monitoring using electrical impedance spectroscopy [7] and non-invasive monitoring of apoptosis using ultrasound backscatter microscopy (UBM) [8]. Detection of apoptosis in cell pellets after PDT using optical coherence tomography (OCT) has also been reported by van de Meer *et al* [9]. In this paper, we describe ongoing development/evaluation of UBM and OCT to monitor the various tissue responses caused by PDT.

Apparatus

Similar to clinical ultrasound systems, UBM forms an image by detecting reflected or backscattered ultrasound from subsurface boundaries caused by variations in density and/or compressibility of tissues. By using higher frequency transducers, UBM has much finer spatial resolution than clinical ultrasound and can achieve microscopic cross-sectional imaging. The UBM system (Visual Sonics, Toronto, ON, Canada) used in this work is an improved version of that previously described [10]. A 40MHz concave PVDF transducer (focal length = 9 mm, F# = 2.2) is mounted on an x-y-z translation stage for tomographic imaging. The frame rate for an 8 mm (depth) × 8 mm (lateral) image is ~ 4 frames per sec (fps). The focal spot size is approximately 70 μm in diameter. The transducer is excited by a single cycle of 40MHz pulse, corresponding to an axial spatial resolution of ~ 38 μm in tissue. The detected ultrasound backscatter signal can be digitized directly by a high-speed A/D converter at 500MHz (8-bit) for ultrasound backscatter spectroscopy (UBS) or be demodulated first and digitized at 50MHz (10-bit) for imaging (e.g., B-mode). A layer of coupling medium (gel or water) is inserted between the transducer and tissue during scanning. The dynamic range of the system is ~ 80 dB. The typical signal to noise ratio (SNR) is ~ 50 dB in UBS mode and ~ 60 dB in B-mode. When performing spectroscopy, the transducer is parked at selected locations to collect 25 to 36 A-scans, thereby improving the SNR by averaging.

Analogous to UBM, OCT uses backscattered infrared light from subsurface boundaries caused by variations in optical refractive index and also forms subsurface cross-sectional images. A functional extension of OCT is optical Doppler tomography (ODT) to detect blood flow, similar to Doppler ultrasound. For this work, OCT and ODT are performed using a recently developed phase-resolved OCT system [11] with 10 μm resolution in both the axial and lateral directions. A broadband light source at 1300 nm with 62 nm bandwidth (coherence length ~ 10 μm in tissue) is coupled into a single mode fiber. The polarized output power exiting the fiber is ~ 5mW. A modified Michelson interferometer (50/50 split ratio) with a fiber optic circulator is used to split the light into the sample arm and the reference arm. A balanced-photodetector (dynamic range ≈ 65 dB, bandwidth ≈ 10 MHz) and a coherent demodulator (dynamic range ≈ 75 dB, bandwidth ≈ 1.6 MHz) are used to detect the interference signal. On-line digital signal processing is performed on a personal computer after 12-bit A/D conversion at 5 MHz. Depth scanning (A-scan) is accomplished with a rapid-scanning-optical-delay line (RSOD) at 8 kHz in the reference arm. In the sample arm, the light is focused to 10 μm diameter and scanned laterally by a motorized linear translation stage with a maximum speed of 6 mm/s. The frame rate for 1 mm (depth) × 3 mm (lateral) field of view is ~ 1 fps for structural OCT imaging. For Doppler imaging, the lateral scanning speed is reduced to 1 mm/s to minimize velocity noise. The Doppler shift due to moving blood is calculated using the

Kasai velocity estimator and the tissue motion artefact is removed using a histogram segmentation technique [11]. Eight sequential scans are averaged in these digital processing algorithms to reduce velocity noise, achieving a Doppler shift detection limit of ~ 100 Hz that corresponds to ~ 30 μm/s flow rate (axial). The detectable Doppler shift range is ± 4 kHz for bi-directional flow before velocity aliasing occurs, corresponding to ~ ± 5 mm/s maximum detectable flow (for Doppler angle = 75º).

Material and Methods

- *In vivo* Experiments:

A human melanoma cell line (ATCC HTB-67) was propagated in modified Eagle's medium with 10% FBS. Approximately 10^4 cells were injected intra-dermally into the hind leg of male SCID mice. A pigmented tumor of ~ 5 mm in diameter was visible after 4 weeks. At 20 ~ 24 hours after i.p. injection of 10 mg/kg of Photofrin (QLT), 5J/cm^2 of 532 nm laser light was administered as a surface irradiation through the overlying skin under general anaesthesia. Both imaging modalities (UBM/UBS and OCT/ODT) were performed between 0 and 20 hours after the light irradiation. Upon sacrifice at 20 hours, the tumor was resected in whole for histology.

- *In vitro* Experiments

(1) Spheroids:

Glioblastoma (GBM) cells were grown into spheroids of ~ 1.5 mm in diameter. The spheroids were randomly selected into the treatment and control groups. For the treatment group, the spheroids were incubated with 10 mg/kg Cisplatin in phosphate buffered saline (PBS) for 15 minutes, washed, and re-incubated with growth medium for 0, 3, 6, 12, 16 and 20 hours. OCT measurements were made at each of the time points. At each time point, a group of 3 spheroids from each of the treatment and control group was imaged, and then placed in 10% Formalin for immunohistochemistry. Chromogenic TUNEL assay and H&E staining are performed after 48 hours for identifying apoptosis.

(2) Pellets:

To investigate the UBM and OCT changes due to DNA packing, AML-5 leukemia cells were exposed to Butyrate at 5mM for 3 days, which acts on DNA-associated histone and reduces DNA packing. The nuclei were then extracted and pelleted in PBS for imaging. To explore the contribution of cell membrane changes to the signal intensity of UBM and OCT, bovine red blood cells (RBC) were exposed to 75% saline for ~ 10 minutes, which caused the cells to swell (~ 10% lysed). The RBCs were then pelleted in PBS for imaging. Finally, whole AML cells were pelleted in PBS (i.e., growth factors and medium removed) so that they underwent natural apoptosis over 24 hours. This allows monitoring of the time course of the apoptosis process without changes in the detector to sample geometry.

Results

- *In vivo* Experiments:

A typical set of results from UBM/UBS and OCT/ODT are shown in Fig. 1. The OCT/ODT measurements were performed first to avoid confounding changes in blood flow due to hypothermia caused by wetting the tissue surface by the ultrasound coupling

medium (gel or water). In agreement with previous experiments, the UBM image of the treated melanoma was brighter (intensity 115 ± 15 a.u.) at 20 h post PDT in compared to that at 3 h (intensity 85 ± 15 a.u., see Fig. 2). Similarly, the UBS at 20 h contained more high frequency components than at 3 h, suggesting a decrease in the effective diameter of the ultrasound scatterers. In Fig. 3, the OCT/ODT images acquired at 4 different time points post PDT are compared. The apparent OCT image intensity of the tumor decreased shortly after PDT, and this trend persisted up to the 7 h. At 20 h, the signal intensity recovered to comparable levels to that at 3h. This suggests an increase in the total attenuation coefficient (μ_t) followed by a decrease. This is in agreement with the *in vitro* spheroid experiments. A concurrent change in blood flow pattern was seen, as shown in Fig. 3, where the both the blood flow velocity and the blood vessel diameters increased from the 3 h to 7 h post PDT. This suggests a transient increase in micro-perfusion. At the 20 h, the perfusion is obliterated, suggesting haemostasis and possible vascular damage.

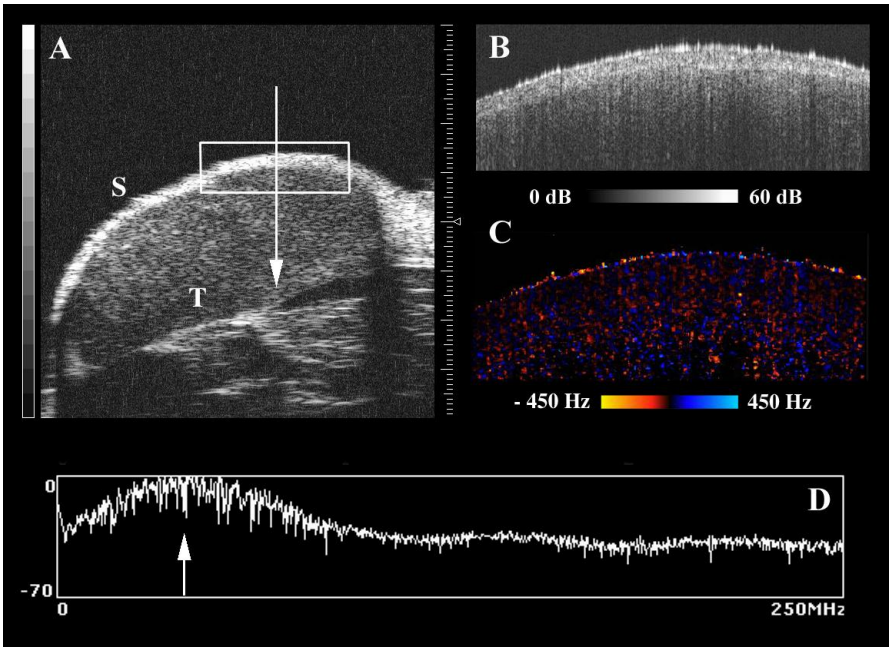

Fig. 1. Typical results of melanoma *in vivo*: (A) UBM image (8 × 8 mm). S-skin; T-tumor. The rectangle indicates an 1 × 3 mm area imaged by OCT (B) and ODT (C). Vertical bands in (B) are shadow artefacts due to bright reflections at the surface. The measured noise level in (C) is ~ 100 Hz and no apparent blood vessels are visible in this particular image. (D) UBS performed along a selected A-scan location indicated by the arrow in (A). The arrow in (D) indicates the center frequency (40 MHz) of the ultrasound transducer.

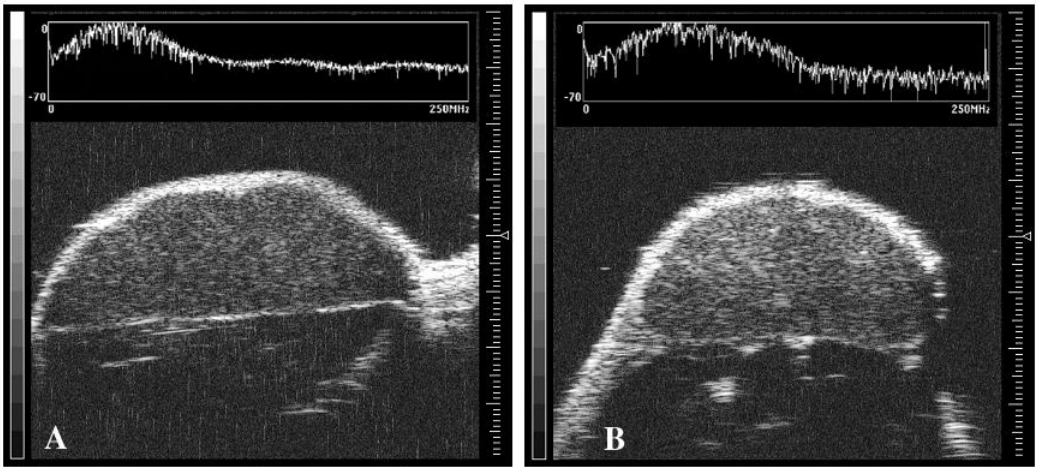

Fig. 2. Comparison of *in vivo* UBM and UBS at 3 h (A) and 20 h post PDT (B). Since a 532 nm laser was used in the PDT, treatment depth is ~1-2 mm. At ~ 1 mm below the skin surface, five areas of 0.5 × 0.5 mm are chosen at random and the average UBM signal intensity is ~ 85 ± 15 (a.u.) in (A). The corresponding signal intensity in (B) is ~ 115 ± 15, in agreement with the brighter visual appearance. The UBS contains more high frequency components at 20 h than 3 h post PDT. Image size: 8 × 8 mm.

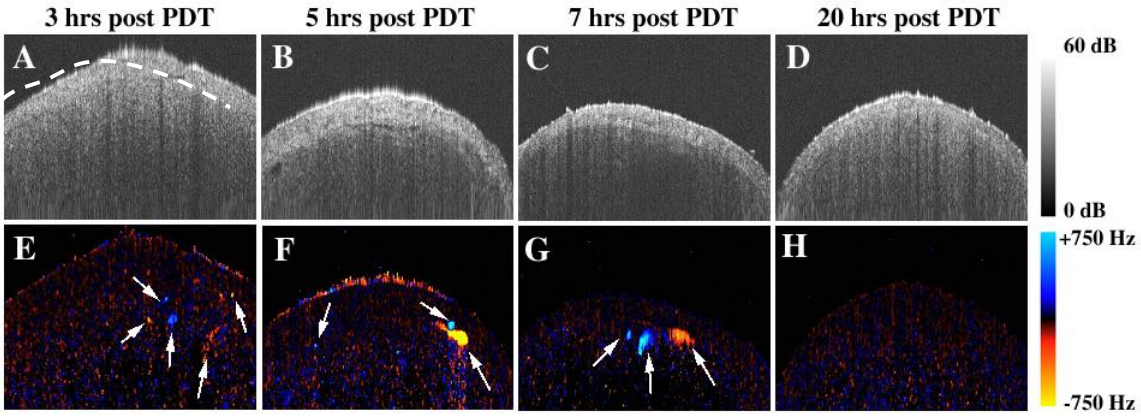

Fig. 3. Comparison of OCT and ODT *in vivo* at various time points after PDT. A-D: OCT images showing the melanoma (under the dash-line) and the skin (above the dash-line). Notice the decreasing OCT signal intensity from A to C, and the recovery of signal in D. E-H: Corresponding ODT images showing the neovasculature (prominent blood vessels are marked by arrows). Notice the apparent increasing blood flow and vessel diameters from E to G, and the obliteration of blood flow in H. Image size: 1 × 3 mm.

In summary, we observed the following changes *in vivo* post PDT: (a) an increase in the ultrasound backscatter intensity; (b) an increase in the high frequency portion of the ultrasound backscatter spectrum; (c) a transient increase in the optical attenuation; and (d) a transient increase in the neovasculature blood flow followed by obliteration of perfusion. An experiment with a larger series of animals (n=25) is currently underway to confirm these preliminary findings.

- *In vitro* Experiments

(1) Spheroids:

The transient increase in the optical attenuation observed *in vivo* post PDT is in agreement with the *in vitro* spheroid experiment, where apoptosis was induced by Cisplatin treatment. As shown in Fig. 4, there was an increase in the total attenuation immediately after Cisplatin incubation, with a peak (~50% higher than that of the control group) occurred at the first time point (3h). This transient increase is statistically significant (95% level, t-test=2.37).

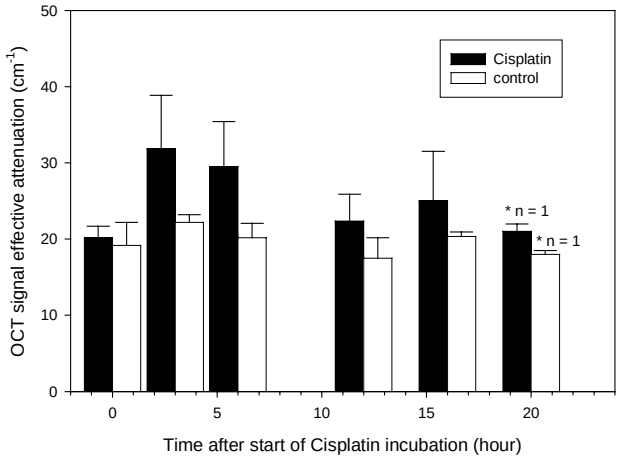

Fig. 4. Changes in the optical total attenuation as measured by OCT in Cisplatin treated and control spheroids. At 3 h post treatment, when the observed difference in average total attenuation is maximum, t-test shows statistical significance at 95% confidence level (t = 2.37*). n = 3 for all data points except last two (*).

(2) Pellets:

As shown in Fig. 5, the UBM signal intensity was reduced in the treated DNA while the OCT intensity increased. The UBM signal from the RBC was much weaker than that from the nuclei, and the signal increased after the 75% saline treatment, whereas the opposite was true for the OCT signal. Finally, there was a marked increase in the UBM signal intensity in the apoptotic AML cells, and a small decrease in the OCT intensity was observed.

Discussion and Conclusions

PDT can induce a variety of tissue changes, including apoptosis, oncosis, and vascular response. In the preliminary *in vivo* animal experiment, an increase in the UBM intensity and a decrease in OCT intensity were observed after PDT, in agreement with previous experiments [8,10]. It is probable that the Photofrin PDT induced a mixed tissue response, including both oncosis and apoptosis, as well as vascular responses. Apoptosis involves nuclear condensation and the formation of apoptotic bodies. The fragmented DNA formed may introduce small scattering centers of higher density than the

surrounding cytoplasm. This may translate into changes in the local density and index of refraction. In addition, the mechanical property of fragmented DNA is probably different from intact long strands of chromatin, inducing changes in the local compressibility. Although these changes are occurring on a sub-cellular length scale, the associated change in the distribution of scattering centers during apoptosis can lead to change in the speckle pattern and ultimately lead to changes in the signal intensity (and/or spectrum), for both the UBM and OCT. The DNA + Butyrate experiment supports such hypothesis, since the reduced DNA packing after Butyrate treatment caused the UBM and OCT signal to change in the opposite direction from apoptosis. In the case of OCT, this is further supported by the results in spheroids treated by Cisplatin. Finally, as the RBC experiments suggested, the UBM signal arises primarily from the backscattering of ultrasound energy due to the nuclei, since the RBC signal intensity is orders of magnitude lower than that from the nuclei or whole cells. This is not true for OCT where the signal contributions from the nuclei and the membrane are probably comparable. To date, the changes observed by UBM and OCT are in the opposite direction. This is not surprising due to the different physical processes involved (acoustics vs optics). Both imaging modalities are still in the demonstration stage; however, for PDT monitoring, the choice of modality will probably depend on the clinical application. For example, in the treatment of acute macular degeneration, where most of the PDT response is believed to be vascular, OCT/ODT should be used since it has a much better velocity resolution and is more suitable for observing microvasculature in the eye. For other solid tumors, the reverse might be true, since the UBM/UBS technique has much better penetration depth and appears to have the capability of monitoring apoptosis.

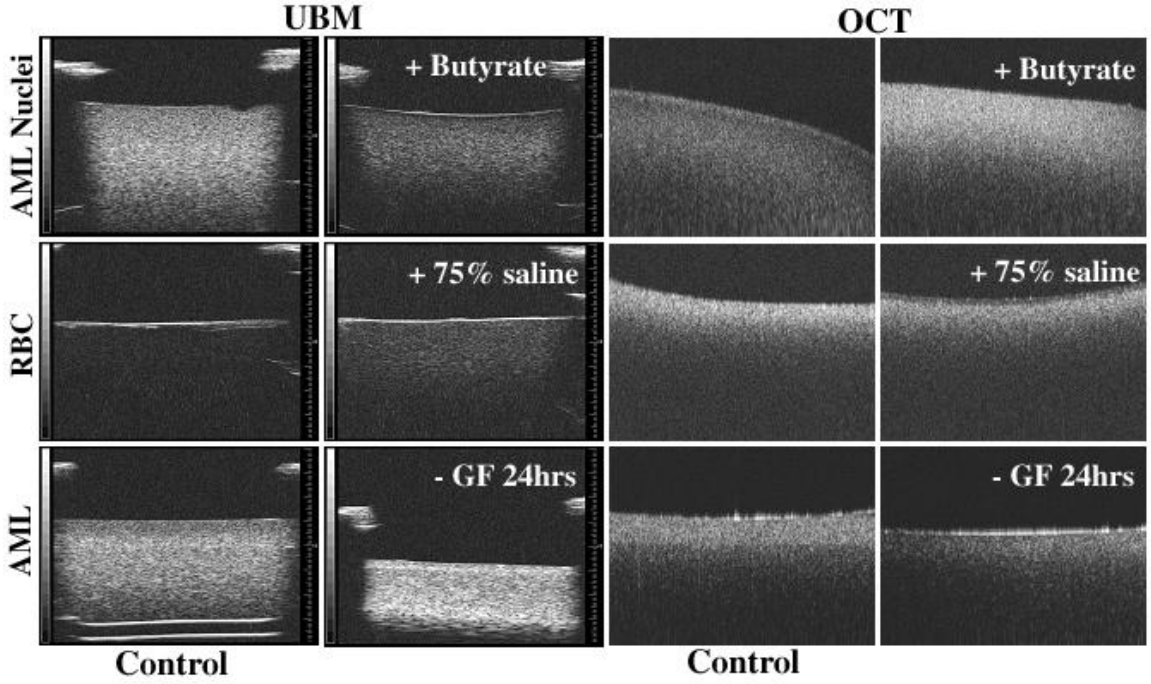

Fig. 5. Comparison of UBM (8 × 8 mm) and OCT (1 × 3 mm) *in vitro* experiments using pellets of AML cell nuclei, RBC, and AML cells. The gain was identical for all images of the same type of imaging modality. Notice that the image intensity is the logarithmic of the received signal amplitude.

In summary, these preliminary results suggest that UBM/UBS can detect PDT-induced tissue changes, including apoptosis. ODT is very sensitive to changes in microvasculature, and PDT-induced vascular response can be detected. Further work is required to confirm these findings and extend them to other *in vitro* and *in vivo* models.

Acknowledgements

This work is supported by the Canadian Cancer Society through a grant from the National Cancer Institute of Canada. Instrument development was supported by the Natural Science and Engineering Research Council (Canada), Photonics Research Ontario, and the Canadian Institute for Health Research. The authors thank the Beckman Laser Institute for collaboration on the spheroid work. Inspiring discussions with Alvin Yeh and Zhongping Chen are appreciated. We also thank Chun Ho Sun and Anoja Giles for help with the biological experiments.

References:

1. Stewart F, Baas P, and Star W, What does photodynamic therapy have to offer radiation oncologists (or their cancer patients)?, *Radiother. Oncol.* 48:233-48, 1998.
2. Colussi V C, Feyes D K, and Mukhtar H, Perspectives of photodynamic therapy for skin diseases, *Skin Pharmacol. Appl. Skin Physiol.* 11:336-46, 1998.
3. Rivelles M J and Baumal C R, Photodynamic therapy of eye diseases, *Ophthalm. Surg. Lasers* 30:653-61, 1999.
4. McIlroy B W, Spectroscopic studies of photodynamic therapy related to real-time monitoring of dosimetry, PhD thesis, University College London, UK, 1998.
5. Lilge L, Portnoy M, and Wilson B C, Apoptosis induced in vivo by photodynamic therapy in normal brain and intracranial tumor tissue, *Br J Cancer*. 83(8):1110-7, 2000.
6. Pogue BW, Braun RD, Lanzen JL, Erickson C, Dewhirst MW, Analysis of the heterogeneity of pO2 dynamics during photodynamic therapy with verteporfin, *Photochem. Photobiol.* 74(5):700-6, 2001.
7. Molckovsky A and Wilson B C, Monitoring of cell and tissue responses to photodynamic therapy by electrical impedance spectroscopy, *Phys. Med. Biol.* 46:983-1002, 2001.
8. Czarnota G J, Kolios M C, Abraham J, Portnoy M, Ottensmeyer F P, Hunt J W, and Sherar M D, Ultrasound imaging of apoptosis: high-resolution non-invasive monitoring of programmed cell death *in vitro*, *in situ*, and *in vivo*, *Br. J. Cancer*, 81:520-7, 1999.
9. van de Meer F J, Faber D J, Aalders M C, van Leeuwen T G, Detection of apoptosis by optical coherence tomography, *Proc. SPIE* 4251:28, 2001.
10. Sherar M D, Noss M B, and Foster F S, Ultrasound backscatter microscopy images the internal structure of living tumour spheroids, *Nature* 330:493-5, 1987.
11. Yang V, Gordon M, Mok A, Zhao Y, Chen Z, Cobbold RSC, Wilson B, Vitkin A, Improved phase-resolved optical Doppler tomography using the Kasai velocity estimator and histogram segmentation, *Opt. Comm.* (in press) 2002.